Part I.

IONOSPHERIC *h'f*-OBSERVATIONS OBTAINED DURING THE PERIOD OF THE SOLAR ECLIPSE OF 30th JUNE 1954

BY

B. LANDMARK, F. LIED, and S. SKRIBELAND

Norwegian Defence Research Establishment

(Manuscript received 7th October 1955)

Abstract: During the solar eclipse of 30th June 1954 ionospheric measurements were made by the NDRE at three different stations, and in this report the *h'f*-observations are described and the results analysed.

In interpreting the results it is assumed that only the recombination of the free electrons is of importance, and consequently de-ionization by other mechanisms is not taken into account.

With these assumptions it is shown that the obtained results cannot be explained in terms of a uniform distribution of the ionizing agency over the sun's disc, and a solar model has been postulated to give a better agreement with observed and calculated curves. Values of the recombination coefficient α have been deduced for E-, F_1- and F_2-layers.

With regard to the F_2-layers it is found that at a period around maximum eclipse the observations can only be explained in terms of a marked solar control of the ionizing agency. A smaller dip observed at all three stations some time before the optical eclipse, may possibly be explained in terms of a corpuscular eclipse.

1.0 INTRODUCTION AND OUTLINE

Considerable interest is attached to the effects of a solar eclipse on the electron densities of the ionized layers. As the radiation from the sun causes the ionospheric layers, the indirect observation of the ionization through radio measurements provides information about the solar ionizing radiation, and may also provide information about physical processes at work in the upper atmosphere.

The fundamental differential equation, giving the balance between the production and loss of electrons during a solar eclipse, is

$$\frac{dN}{dt} = p(t)\ q_o \cos\varkappa - \alpha N^2, \qquad (1.1)$$

where N is the number of free electrons per unit volume, $q = q_o\, p(t) \cos\varkappa$ is the number of free electrons produced per unit volume per unit time, α is the effective recombination coefficient, $\varkappa$ the zenith angle of the sun, and $p(t)$ is the fraction of the ionizing radiation unobscured.

If one assumes the ionizing radiation to be uniformly distributed over the sun's disc, $p(t)$ gives the fraction of the sun's disc unobscured. In this case it is possible from equation (1.1) to compute N/N_o, as a function of time for different values of α, N_o being the value of N at first contact. A comparison of the theoretical curves with the experimental one should allow α be determined, and once this parameter is determined, q_o is also obtained from N_o. Earlier eclipse observations have shown that it is impossible to obtain a very good fit between the observed $N(t)$ curve and the theoretical curves for any values of α and it is concluded by different workers that this must be due to a non-uniform distribution of the ionizing radiation over the sun's disc.

The total solar eclipse of 30th June 1954 occurred during a period of extremely low solar activity, and according to a report from the High Altitude Observatory at Boulder, Colorado [1] «it will probably rank as the lowest activity eclipse of modern times. It was a time when the disc was devoid of sunspot and plages, and coronal emission visible in the coronagraph had almost completely disappeared. There was no green line (5303A) emission visible on either the Climax or Sacramento Peak spectrograms on that day, but there was some low intensity red line (6374A) emission».

During the period of the eclipse, ionospheric measurements were made by the NDRE at three stations.

Station	Geographical coordinates	Max. obscuration at ground
Tromøya	58° N, 9° E	99.5 %
Kjeller	60° N, 11° E	99,0 %
Tromsø	70° N, 19° E	75,4 %

At Kjeller 96 % of the sun's disc was obscured at a height of 120 km, at Tromøya the eclipse was total for about 2 minutes and 39 seconds at the same height, and at Tromsø 66.4 % of the sun's disc was obscured again at the same height.

In section 2 of this report the $h'f$-measurements carried out during the eclipse period are reported.

The interpretation of the results for the E- and F_1-layers is given in section 3. Interpretation in terms of uniform radiation over the sun's disc has been attempted, but the conclusion is that even for this eclipse, which occurred when the sun was extremely quiet, this assumption is not satisfactory. In order to explain the variation of the electron density N in the E- and F_1-layers observed at the three stations, a new solar model has been adopted. This solar model is compared with the results of optical observations of the sun, and the uniqueness of our interpretation is briefly discussed.

The results for the F_2-layers are discussed in section 4, and it is shown that the observations can only be explained in terms of a marked solar control of the ionizing agency, and that the value of the recombination coefficient must be quite large. The results are also compared with observations made by other investigators. In section 5 the conclusions of the investigations are summarized.

2.0 OBSERVATIONS

During the eclipse the following ionospheric measurements were made by the NDRE at the three stations:

Tromøya......	$h'f$-recordings absorption measurements
Kjeller	$h'f$-recordings absorption measurements E-layer wind measurements long wave measurements
Tromsø	$h'f$-recordings long wave measurements

The results of the absorption measurements are given by Lied and Orhaug as Part II of this communication, and the results of the E-layer wind measurements are given by Harang and Pedersen [2] in an internal report. The long wave measurements were made as part of a programme drawn up by the radio group at the Cavendish Laboratory, and we have not made a detailed analysis of the result. However, the observations have been given in an internal report [3].

2.1 Programme of measurements.

During a control period consisting of 5 days before and 5 days after the day of the eclipse $h'f$-recordings were made every quarter hour at the three stations. The records obtained were of the normal type, covering a frequency range from 0.7 to 24 Mc/s, each recording being obtained on 7 cm paper in 5 minutes using NPL-recorders.

Between 0900 MET and 1700 MET on the day of the eclipse more frequent observations were taken. At Tromsø one recording was taken every 4th minute, covering a frequency range from 0.7 to 7.0 Mc/s. At Kjeller and Tromøya one time marked recording covering the frequency range 0.7—7.0 Mc/s was followed by two conse-

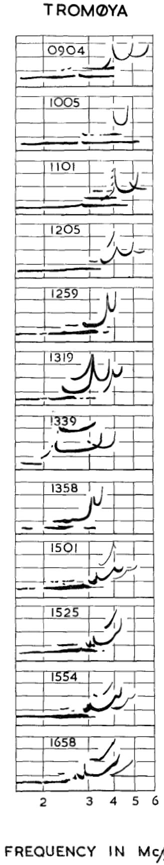

n records obtained at the three stations

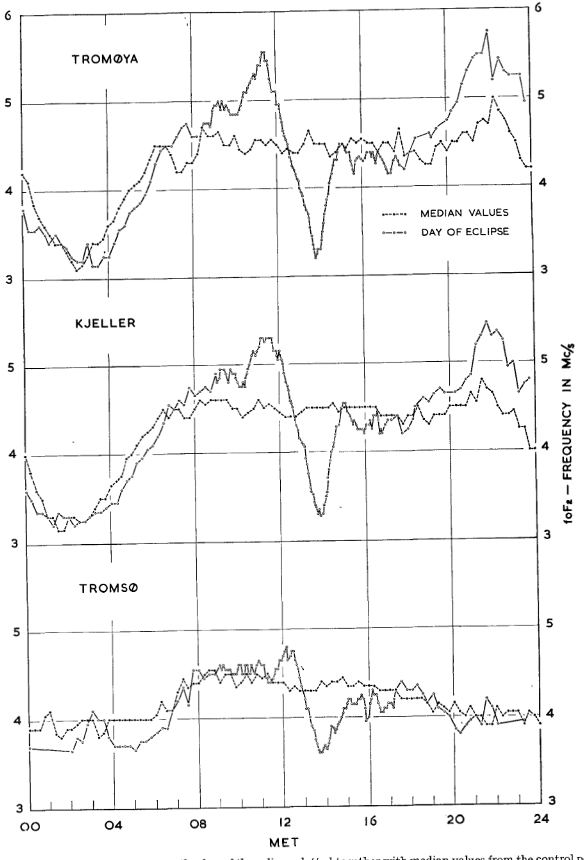

Fig. (2.2) Observed values of *foF2* on the day of the eclipse plotted together with median values from the control period.

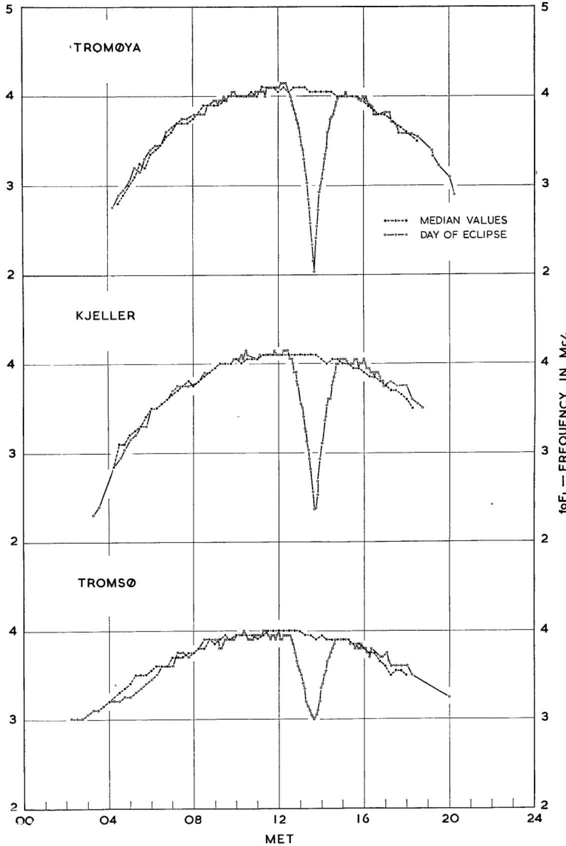

Fig. (2.3) Observed values of *foF1* on the day of eclipse plotted together with median values from the control period.

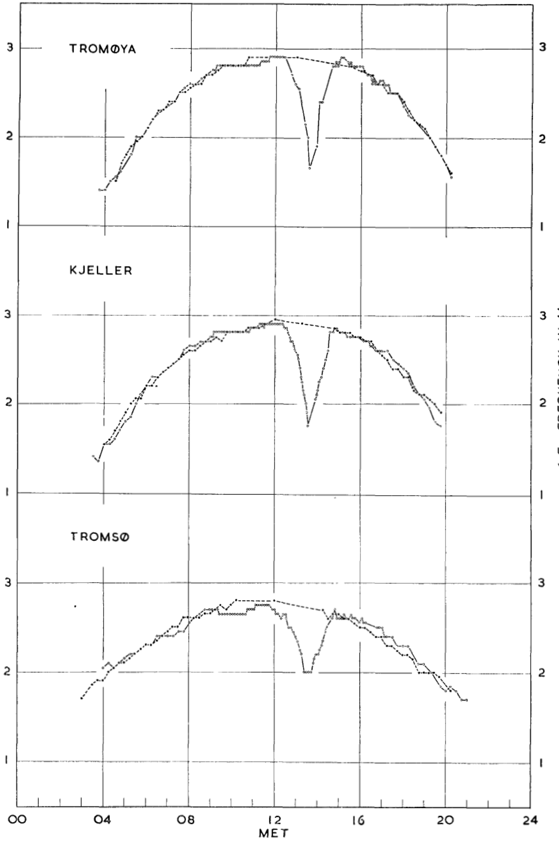

Fig. (2.4) Observed values of foE on the day of the eclipse plotted together with median values from the control period.

cutive records covering the frequency range 1.4—7.0 *Mc/s*.

The reason for choosing a different programme at Tromsø than at the other stations was that at Tromsø no absorption measurements were made, and it was felt that it would be of interest to obtain frequent observations of f_{min}.

Each recording was carefully timed, and it has been possible to determine the critical frequency times with an accuracy of $\pm$ 1 second.

2.2 Observational results.

The results are presented in the form of tables and curves, and the measured parameters are shown together with median values from the control period. The measured critical frequencies for the E-, F_1- and F_2-layers for the three stations for the period between 0900 *MET* and 1700 *MET* of 30th June are given in Tables 2.1 to 2.9 at the end of this report, together with the exact times at which these frequencies were measured.

In Fig. (2.1) sample redrawn records are shown for the three stations. It will be observed from these records that a marked decrease was observed for the critical frequencies for the E-, F_1- and F_2-layers during the eclipse. Furthermore a very close similarity is evident between the records obtained at Kjeller and at Tromøya, and also to some degree between these and the records obtained at Tromsø. Heavy E_s-ionization was observed at all three stations, and it has therefore been difficult to determine *foE* with any very large degree of certainty.

In the F_1-layer a «two-ledge» phenomenon was observed at Tromøya and Kjeller in the late phase of the optical eclipse period. From these the lower value was always chosen as *foF1*.

In Fig. (2.2) the measured critical frequencies for the F_2-layers at the three stations for the day of the eclipse are shown together with median values from the control period. The critical frequencies for the E- and F_1-layers are shown in the same way in Figs. (2.3) and (2.4).

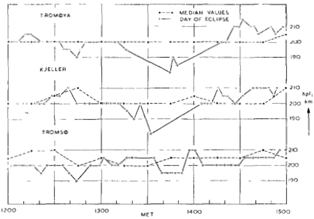

Fig. (2.5). Observed values of *hpF1* on the day of the eclipse plotted together with median values from the control period

It is obvious from Fig. (2.1) that $h'F_2$ has been very much influenced by group retardation in the F_1-layer during most of the eclipse period, and a study of $h'F_2$ therefore will give little information about the variation in true height of the F_2-layer. The measured values of $h'F_2$ have been plotted (these curves are not included in this report) and a very close correspondance is found between the values obtained at Tromøya and at Kjeller. This effect is also evident in Fig. (2.1).

In Fig. (2.5) the observed values of *hpF1* for the day of the eclipse have been plotted together with median values from the control period. It seems that there is a tendency for the value of *hpF1* to decrease slightly around maximum eclipse, but it was possible to obtain only a few values of *hpF1* for this period.

3.0 PHYSICAL INTERPRETATION FOR E- AND F_1-LAYERS

For the E- and F_1-layers it is generally assumed that nearly all, if not all, of the ionization occurring is due to radiation from the sun's disc. By measuring variations of electron density in the layers, it should therefore be possible to deduce both the distribution of the ionizing agency over the sun's disc and the recombination coefficient α in these layers.

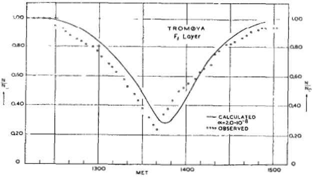

Fig. (3.1). Calculated and measured N/N_0 for F_1-layer at Tromøya.

Equation (1.1),

$$\frac{dN}{dt} = p(t)\, q_0 \cos \varkappa - \alpha\, N^2, \qquad (3.1)$$

is valid in this form when only the recombination of the free electrons is taken into account. If the combination of free electrons and neutral atoms is of importance, another term must be included in equation (3.1) to account for this mechanism. It is also assumed that the rate of generation of electrons q may be written as $q_0 \cos\varkappa$. This assumption is justified if the observed critical frequencies during the control period follow a cosine 1/4 law. This has not been found to be completely the case, but since the eclipse occurred very nearly at local noon both at Tromøya and Kjeller, and since the $\cos \varkappa$-term is consequently nearly constant, the agreement is quite good. At Tromsø which is a more easterly station a disagreement occurs in the late phase of the eclipse period, and here a better approximation would probably be obtained by assuming the $\cos \varkappa$-term to be a constant throughout the eclipse period.

3.1 Interpretation in terms of uniform radiation over the sun's disc.

As the solar eclipse in question occurred at approximately local noon both at Tromøya and Kjeller, and since the observed variations in the values of *foE* and *foF1* at Tromsø indicate a constant $\cos\varkappa$-term in the eclipse period, we may neglect the variations of $\cos \varkappa$ in equation (3.1). In this case the equation may be written.

$$\frac{1}{\alpha N_0}\frac{dy}{dt} - y^2 = p(t), \qquad (3.2)$$

where $N_0 = \sqrt{q_0 \cos \varkappa / \alpha}$ is the maximum electron density in the layer in question at first contact, and $y = N/N_0$.

From equation (3.2) it is possible to calculate the theoretical $N(t)$-curves for the different layers at each station, and for differing values of the recombination coefficient α. This has been done for Kjeller and Tromøya with $p(t)$ calculated for a height of 120 kilometers. Since the $p(t)$ curves for these stations at a height of 200 kilometers differ very little from the curves for 120 kilometers, the calculated $N(t)$-curves can be used for both the E- and F_1-layers. The conclusion drawn from these calculations is that it is impossible to obtain a good fit between the observed and calculated $N(t)$-curves for any value of the recombination coefficient α, and the effect is illustrated in Fig. (3.1) where the calculated and observed $N/N_0(t)$-curves are shown for the F_1-layer at Tromøya. The calculated curve is for $\alpha = 2\cdot10^{-8}$

The disagreements evident in Fig. (3.1) between the theoretical curve and the observed curve are typical for both E- and F_1-layers at all three stations, and we are of the opinion that they are typical for all ionospheric measurements hitherto made during solar eclipses. It has been customary to determine α from (i) the phase lag between maximum eclipse and observed minimum of the electron density, (ii) the minimum value of the electron density and (iii) the overall fit between observed and theoretical curves. We felt that these techniques are of little value because it appears

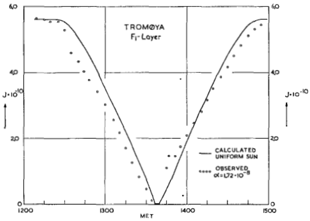

Fig. (32.). Comparison between the theoretical J-curve assuming uniform radiation from the sun's disc and curves obtained from measurements.

that measured variations of the electron density cannot be explained in terms of uniform radiation from the sun's disc.

3.2 Interpretation in terms of non-uniform radiation over the sun's disc.

Considering again equation (3.1) which may be written,

$$J(t) = \frac{q_o}{a} p(t) = \frac{1}{\cos \varkappa} (N^2 + \frac{1}{a} \frac{dN}{dt}) \quad (3.3)$$

we see that if a is a constant and dN/dt may be determined from the observed $N(t)$, $J(t)$ which is proportional to $p(t)$ may be determined from the observations for different values of the parameter a.

As the determination of the critical frequencies for the E-layers has proved extremely difficult because of the heavy E_s-ionization, most of the values of foE are doubtful values. The E-data is therefore not suitable for analysis. The F_1-data, on the other hand, is reliable, and the $N(t)$-curves from these layers can be differentiated.

By assuming all ionizing radiation to be limited to the sun's disc, the recombination coefficient may be determined from the period during which the eclipse was total at Tromøya. During this period $p(t) = 0$, and consequently,

$$a = -\frac{dN/dt}{N^2}. \quad (3.4)$$

The recombination coefficient as determined by this technique, from the Tromøya observations gives the value

$$a_{F1} = 1.72 \cdot 10^{-8}.$$

In Fig. (3.2) the experimental J-curve for the F_1-layer at Tromøya is shown (circles). This curve differs markedly from the J-curve obtained by assuming uniform radiation over the sun's disc (drawn). The disposity between the curves at first and third contact may be explained by assuming approximately 16 % of the radiation at the Western limb of the sun. The discrepancy at second and fourth contact may be explained by assuming approximately 4 % of the radiation at the Eastern limb of the sun. Furthermore, in order to obtain a good fit between calculated and observed J-curves, approximately 16 % of the radiation must be assumed in the middle part of the sun.

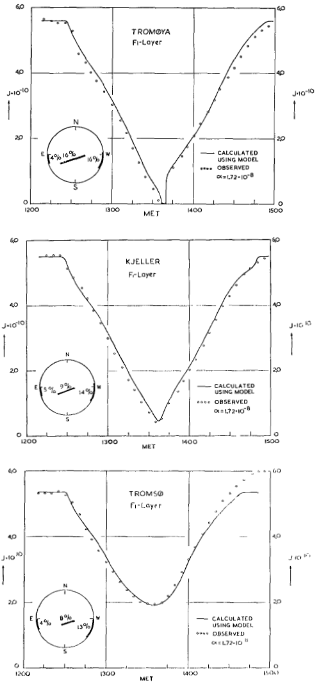

Fig. (3.3). Comparison between the theoretical J-curves and the curves obtained from measurements. $a = 1.72 \cdot 10^{-8}$.

In Fig. (3.3) the J-curves obtained for the three stations by standard techniques of smoothing and differentiating the $N(t)$-curves for $a = 1.72 \cdot 10^{-8}$ for the F_1-layers (circles), are given together with theoretical J-curves obtained by assuming different solar model.s The value of a, $a_{F1} = 1.72 \cdot 10^{-8}$,

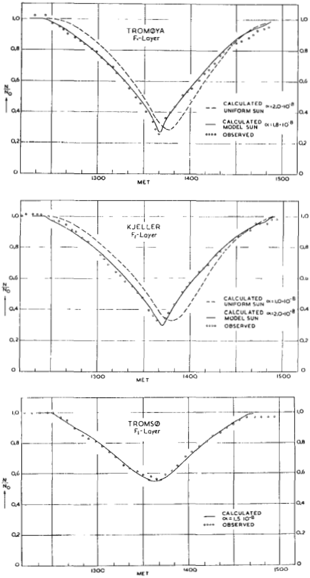

Fig. (3 4). Observed and calculated N/N_0-curves for the F_1-layers.

as determined from the period of total eclipse at Tromøya, gives an upper limit for α_{F1}. For values of α less than this value, the observed J-curve would become negative. On the other hand greater values of α are possible, and this point is discussed in some detail in section (3.4).

As the three solar models adopted from F_1-observations at the three stations prove to be reasonably similar, we have assumed a common solar model determined in such a way as to give best fit between observed and theoretical curves at the three stations at the same time. This model is shown in Fig. (3.4) where it is compared with results obtained by optical observations of the sun.

Using $p(t)$-curves determined from this solar model the differential equation in the form (3.2) has been solved for ditferent values of the parameter αN_0. In Fig. (3.4) the results of this analysis are shown for the F_1-layer. Values of N/N_0 observed are shown with the theoretical curves obtained using the curves obtained from the model and by assuming uniform radiation. The theoretical curve assuming uniform radiation has not been calculated for Tromsø. It is evident from Fig. (3.3) that a much better fit may be obtained between theoretical and observed curves using the model, than by assuming uniform radiation.

The results for the E-layer are given in Fig. (3.5). Here the values of N/N_0 observed are shown (circles) together with the theoretical curve which follows using the model, and a reasonable agreement is found. It must be borne in mind that nearly all the observed values for N/N_0 are doubtful values.

For each of the curves calculated from the model in Figs. (3.4) and (3.5) the recombination coefficient α is chosen to give the best overall fit between observed and calculated curves. The resulting α-values for the E-layer vary between $1.5 \cdot 10^{-8}$ and $2.0 \cdot 10^{-8}$, and for the F_1-layer between $3.0 \cdot 10^{-8}$ and $4.0 \cdot 10^{-8}$. The corresponding values of q_0 for the E-layer vary between 400 and 530 and for the F_1-layer between 800 and 1100.

3.3 Comparison of "model sun" with the results of optical observations.

The «model sun» which was adopted to give the best fit between observed and calculated J-curves for the F_1-layers at the three stations is shown in Fig. (3.4) together with the results of optical observations of the sun. As mentioned in the introduction, optical observations showed that the eclipse occurred during conditions when the sun was quiet, the only activity being some low-intensity red line coronal emission and a few prominences on the solar limb. In Fig. (3.6) the measured limb-intensity of red line coronal emission is shown, and the position of four small prominences observed is also given.

It follows from Fig. (3.6) that the model postulated, in which 14 % of the total ionizing radiation was placed at the Western limb and 5 % at the Eastern limb, seems reasonable judging by the results of optical observations which showed coronal emission from the same regions. The 10 %

of the total ionizing radiation postulated for the middle part of the solar model cannot be explained in terms of any observed activity. However, this region may cover the greater part of the sun's disc and in fact does not constitute a serious objection to the model.

3.4 Discussion of uniqueness of solution.

As already stated, the value of the recombination coefficient α determined for the period of total eclipse at Tromøya, gives only a lower limit of α_{F1}. There is also the possibility that not all of the ionizing radiation is eclipsed during this period, and it is then necessary to choose a larger

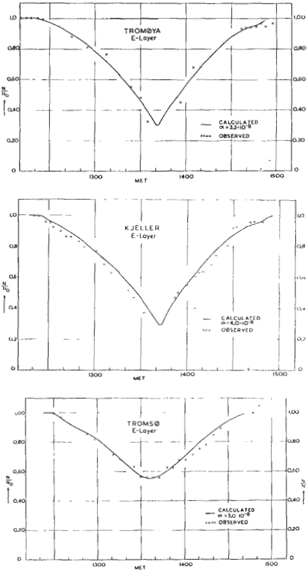

Fig. (3.5). Observed and calculated N/N_o-curves for the E-layers.

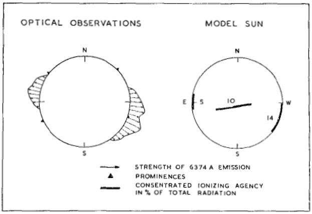

Fig. (3.6). Comparison of «model sun» with the results of optical observations.

value of the recombination coefficient, and to postulate a solar model in order to explain the observed J-curves for this value of α.

Piddington [4] has discussed a number of earlier eclipse observations and has suggested that the value of the effective recombination coefficient is about $5 \cdot 10^{-8}$ in the F_1-layer and $1 \cdot 10^{-7}$ in the E-layer. He has also shown that for these values of α somewhere between 5 % and 20 % of the ionizing agency for the E-layer, and somewhere between 5 % and 10 % of the ionizing agency for the F_1-layer remain unshadowed during a total eclipse, and that this residual agency probably originates in the upper chromosphere and lower corona.

From his observations at Khartoum in 1952, Minnis [5] postulates a solar model in which the disturbances are found to be associated with sunspot and coronal green line emission. He finds that assuming all ionizing agency to be distributed over the sun's disc, α_{F1} and α_E are about $0.8 \cdot 10^{-9}$ and $1.5 \cdot 10^{-8}$. Minnis also develops a method by which q_o can be determined without knowing α, and shows that the values found by Piddington for α_{F1} and α_E would result in values of q_o which are inexplicable.

We have found it impossible to use the same method as Minnis in estimating q_o which is independent of the values of α. We have tried the possibility of starting our interpretation with a larger value of the recombination coefficient, and have been forced to conclude that a reasonably good fit between observed and calculated curves can be obtained even if the value of the recombination coefficient tends towards infinity.

4.0 DISCUSSION OF RESULTS FOR F_2-LAYER

The observed critical frequencies *foF2* at the three stations on the day of the eclipse have been shown in Fig. (2.2) together with median values from the control period. It is obvious that a much higher critical frequency was found generally on the day of the eclipse than in the control period, and that in fact on none of the control days was a frequency observed as high as that on the actual eclipse day between about 0800 and 1200 and between about 1900 and 2400 *MET*. The standard deviation obtained from the control period varies from about 0.2 to about 0.3 *Mc/s*, and the peak observed on eclipse day was about 5 times the standard deviation from the median values obtained during the control period.

From Fig. (2.2) it is obvious that a significant dip in the critical frequency was observed at the times of maximum eclipse at all three stations. It is also noticeable that a smaller dip was observed at all stations some time before the optical eclipse, the significance of this effect being the correspondance between the observed effects at the different stations, rather than any marked departure from the control values.

4.1 The recombination coefficient and responsible ionizing radiation.

The F_2-layer observations are not readily analyzed to give information about recombination in the layers or to give information about the processes responsible for the layers. In the F_2-layer the effective recombination coefficient α is probably much less than in the E- and F_1-layers, and it becomes difficult to interpret the variations of the maximum electron density in the layers in terms of equation (1.1) alone. This is because the variations obtained cannot be explained in terms of a balance between produced electrons and recombined electrons, because random effects, tidal effects and other causes also play a part. Furthermore the interpretation might have to include ionizing agencies other than radiation from the sun's disc.

It follows then that F_2-layer eclipse observations cannot give any accurate determination of the coefficient of recombination α in the layer. Even so, some information may be deduced from such observations. It is at once obvious that the observed decrease during the optical eclipse can only be explained in terms of a marked solar control of the ionizing agency, and that a considerable value of the recombination coefficient is necessary to explain the observed curves.

A rough estimate of α may be obtained from the period around total eclipse if the observed $N(t)$-curves can be differentiated. Rewriting equation (3.3),

$$J(t) = \frac{q_o}{\alpha}\, p(t) = \frac{1}{\cos \varkappa}\left(N^2 + \frac{1}{\alpha}\frac{dN}{dt}\right), \quad (4.1)$$

we assume that the cos $\varkappa$-term is constant in the time interval considered, and that $p(t)$, which gives the fraction of unobscured ionizing agency, may be written as

$$p(t) = c + s(t). \quad (4.2)$$

Here c is a constant term due to ionizing causes other than ionizing radiation from the sun's disc and $s(t)$ accounts for that part of the ionizing agency radiated from the sun's disc.

We observe from Fig. (2.2) that the measured $N(t)$ curve at Tromøya cannot be differentiated, and we consequently consider only the observations made at Kjeller and at Tromsø. For the Tromsø observations a smoothed $N(t)$ curve has been obtained, and from this the values of N^2 and dN/dt have been deduced for each fifth minute in the time period between 1300 and 1430 *MET*. The recombination coefficient has been determined so that the times of minimum of the observed $J(t)$-curve and the minimum of the $s(t)$-curve coincide. This gives a value of the recombination coefficient α of $3 \cdot 10^{-9}$. It is found that the best fit is obtained for $c = 0$ and $q_o = 270$. The observed $J(t)$-curve has been compared with theoretical curves obtained for different values of the constant c and q_o.

In Fig. (4.1) the observed and calculated values for the F_2-layer are shown, those for Tromsø being given on the left. In order to obtain the best fit between observed and calculated curves at Kjeller, the constant term c due to ionizing agency not radiated from the sun's disc, was found to be

0.07, the value of α was found to be $3 \cdot 10^{-9}$ and the value of q_o was found to be 230.

It follows that the observed variations of maximum electron density in the F_2-layer in the period around maximum eclipse may be explained by assuming nearly complete solar control of the ionizing agency, and that the recombination coefficient α in this case has quite a high value, somewhere around $3 \cdot 10^{-9}$. But as already stated, F_2-layer observations during an eclipse do not provide any very reliable information for deducing the recombination coefficient or for examining the mechanism which produces the layers. We feel that it would not be wise to place too much reliance on the results obtained before a more quantitative material is available.

4.2 Comparison of results.

While the E- and F_1-layer observations obtained during earlier eclipses have shown typical variations of the critical frequencies of the type as given in this paper, F_2-layer observations have given very different results. In fact, in some eclipses there has been no change in $foF2$ directly attributable to the eclipse. Berkner [6] in 1939 analyses earlier eclipse observations and says: «The tendency seems to be, that when observations during an eclipse are made where the F_1- and F_2-regions are widely separated, no significant change in ion density of the F_2-region is observed, this situation occurring only in summer in low or middle latitudes.» Our observations which were made in summer at middle and high latitudes, showed a significant decrease of $foF2$, and furthermore a close correspondance was found between the types of variation occurring at the high latitude station Tromsø and the middle latitude stations Tromøya and Kjeller.

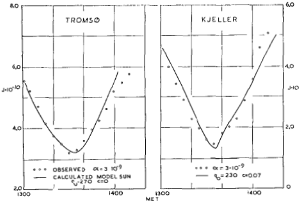

Fig. (4.1). Observed and calculated J-curves for the F_r layer at Tromsø and Kjeller.

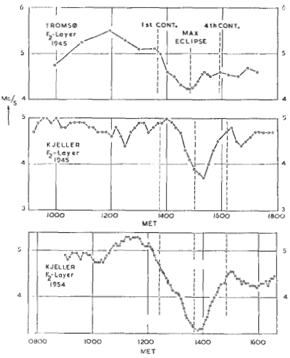

Fig. (4.2). Observed values of $foF2$ at Kjeller and Tromsø during the 1945 eclipse (after Harang), compared with results for 1954 eclipse.

Maeda [7] has plotted the variation in decrease of F_2-ionization against sunspot number for several eclipses, and finds that the decrease is greatest for small values of sunspot number. Our observations fit in well with this result. MacLachlan [8] in 1953 also analysed a large number of eclipse observations, but finds no such regularities.

As already mentioned, a smaller dip was observed for $foF2$ at all three stations some time before first contact. Similar results have been found by various observers, and the effect may possibly be explained as due to a corpuscular eclipse. The significance of the observed dip is not to be found in the departures from the median values obtained during the control period, but in the agreement between the observations at the three different stations and indeed the agreement with other observations.

During the solar eclipse which occurred in Norway in 1945, ionospheric measurements were made at Kjeller and at Tromsø [9]. In Fig. (4.2) the observed values $foF2$ obtained at the two stations during this eclipse have been plotted together with observations from Kjeller in 1954. A comparison between observations made during the eclipses of 1945 and 1954 shows a close correspondance.

Some eclipse observations show a two-layer phenomenon in the F_2-region. Minnis for example observed that after 3. contact at Khartoum in 1952 a new layer is formed between the F_1- and the F_2-layer, which he calls an $F_{1\frac{1}{2}}$-layer. This layer is at first a layer of comparatively low true height and electron density, but these parameters then increase until the layer becomes indistinguishable from the F_2-layer. Our observations did not show any marked effect similar to the one reported by Minnis, but a tendency towards a two-ledge phenomenon was observed in the late phase of the optical eclipse.

5.0 CONCLUSION

It is of interest that during the total solar eclipse of 30th June 1954, which occurred at a period of extremely low solar activity, and which has been characterized as the lowest activity eclipse of modern times, the variations in the electron density of the E- and F_1-layers which were observed cannot be explained in terms of a uniform distribution of the ionizing agency over the sun's disc (see Figs. (3.1) and (3.2)).

The disparities between the calculated and observed curves in Figs. (3.1) and (3.2) show that some part of the ionizing agency appeared to have been concentrated at both the Western and the Eastern limb of the sun. The value used for the recombination coefficient α in calculating the «observed» J-curve in Fig. (3.2) was determined from the period of totality at Tromøya, and thus involves the assumption that all ionizing agency is distributed over the sun's disc.

Because the concentrated radiation from the limbs of the sun also may be due to radiation from the lower corona, and consequently would not be eclipsed at totality, the values deduced for the effective recombination coefficient α can only be regarded as lower limits.

The dip at the period of maximum eclipse which has been observed for the F_2-layer can only be explained in terms of a marked solar control of the ionizing agency, and assuming that our differential equation (4.1) may be used for maximum electron density in the layer, we conclude that at a period around maximum eclipse nearly all the ionizing agency was due to radiation from the sun's disc, and that quite large values of the recombination coefficient are required. As the above assumption is very doubtful, it would not be wise to place too much reliance on these results.

In Table (5.1) given below, are listed the values for the recombination coefficient α, the total rates of generation of electrons q_o and the amount of ionizing agency not distributed over the sun's disc cq_o presented by the values of c as deduced from our observations.

Station	E-layer		F_1-layer		F_2-layer		
	$\alpha \times 10^8$	q_o	$\alpha \times 10^8$	q_o	$\alpha \times 10^9$	q_o	c
Tromøya.....	3.2	420	1.8	1000	—	—	—
Kjeller	4 0	530	2.0	1100	3.0	230	0.07
Tromsø	3.0	400	1.5	800	3.0	270	0

Table (5.1) Resulting values of $\alpha \cdot q_o$ and q/c_o.

The values given show good agreement with values obtained by other investigators from eclipse observations, but they are quite high compared with the generally accepted values.

Acknowledgements.

The investigation described in this paper has been carried out in cooperation with the Auroral Observatory, Tromsø. We are indebted to the Norwegian Research Council for Science and the Humanities for a grant enabling the observations to be carried out at Tromøya and in Tromsø.

We wish to express our sincere thanks to Mr. R. Larsen for his assistance at Tromsø, and to Mr. H. Hoffshagen for his assistance at Kjeller. Valuable assistance from Mr. V. Andreassen has helped us greatly with the work of interpretation and the drawing of illustrations. In the reading of the records great help has been received from Miss I. J. Aarbogh.

The authors also wish to acknowledge a great debt of gratitude to the computing section under the leadership of Mr. J. Garwick, without whose cooperation the interpretation of the results would have been impossible.

References.

[1] Sonnen-Zirkular für die Monate April, Mai, Juni 1954, Veröffentl. des Fraunhofen Instituts, Freiburg I. B.
[2] HARANG, L., and K. PEDERSEN: Internal Report T-101, *NDRE*, Dec. 1954.
[3] BJELLAND, B., B. LANDMARK and F. LIED: Internal Report T-93/172, *NDRE*, August 1954.
[4] PIDDINGTON, J. H.: Journ. Geoph. Res. *56*, p. 409 (1951).
[5] MINNIS, C. M.: Journ. Atmos. Terr. Phys. *6*, p. 91 (1955).
[6] BERKNER, L. V.: Terrestrial Magnetism and Electricity. Ed. J. A. Fleming, New York 1939.
[7] MAEDA, K.: General Headquarters for the Supreme Commander for the Allied Powers in Japan, Civil Communications Section, Research and Development Division, January 6th 1949.
[8] MACLACHLAN, J. H.: Radio Physics Laboratory Project Report 3-0-3, 1953.
[9] HARANG, L.: Geophys. Publ. *16*, No. 11 (1945).

MET h m s	*fo*	*MET* h m s	*fo*	*MET* h m s	*fo*
09 01 29	2.75A	11 40 41	2.85A		A
09 04 21	2.75	11 43 31	2.90 A		A
09 07 11	2.75	11 49 24	2.90 A		A
09 11 36	2.75	11 51 18	2.90 A		A
09 14 28	2.80	11 54 09	(2.90)A		A
09 17 18	(2.80)A	11 57 00	(2.90)A	14 37 40	(2.80)A
09 21 42	2.80	12 01 55	(2.90)A	14 40 30	(2.80)A
09 24 33	2.80	12 04 46	(2.90)A	14 43 20	(2.80)A
09 27 23	2.80	12 07 35	(2.90)A	14 48 12	(2.80)A
09 32 56	2.80	12 12 30	(2.90)A	14 51 03	(2.85)A
09 35 47	2.80	12 15 20	(2.90)A	14 53 55	(2.80)A
09 38 36	2.80	12 18 10	(2.90)A	14 58 48	(2.85)A
09 43 37	2.80	12 23 07	(2.90)A	15 01 39	2.90 A
09 46 28	2.80	12 25 59	(2.90)A	15 04 31	2.90 A
09 49 17	2.80		A	15 09 25	2.90 AF
09 55 02	2.80		A	15 12 27	(2.90)AF
09 57 53	2.80		A		A
10 00 43	2.80		A		A
10 05 06	2.80	12 45 09	(2.70)A	15 22 57	2.85 AF
10 07 57	2.80		A	15 25 46	2.80
10 10 48	2.80		A	15 30 46	2.85 AF
10 15 45	2.80	12 55 47	(2.60)A	15 33 35	(2.80)AF
10 18 35	2.80		A	15 36 26	(2.80)AF
10 21 20	2.80		A	15 41 27	2.80 AF
10 26 22	2.80		A	15 44 19	2.80 AF
10 29 13	2.80	13 09 14	(2.55)A	15 47 10	2.80 AF
10 32 03	2.80		A	15 52 10	2.80
10 37 00	2.80		A	15 55 01	2.80
10 39 50	2.80		A	15 57 52	2.80 A
10 42 40	2.80	13 24 31	(2.15)A	16 02 51	2.80
10 47 35	2.80		A	16 05 40	2.75
10 50 25	2.80	13 30 07	(2.00)A	16 08 30	2.75
10 53 16	2.80	13 34 52	(1.65)A	16 13 31	2.70
10 58 11	2.80		A	16 16 21	2.70
11 02 02	2.80		A	16 19 12	2.70
11 03 54	2.80		A	16 24 12	2.70
11 08 51	2.80		A	16 27 01	2.65
11 11 42	2.80		A	16 29 51	2.60
11 14 32	2.80		A	16 34 50	2.65
11 19 29	2.85	13 58 01	(1.90)A	16 37 39	2.60
11 21 20	2.85		A	16 40 28	2.60
11 25 09	2.85	14 05 44	(2.40)A	16 45 25	2.60
11 30 03	2.85	14 08 34	(2.40)A	16 48 15	2.60
11 32 53	2.85 A		A	16 51 08	2.65 H
11 35 43	2.85 A		A	16 56 08	2.65 H

Table (2.1). Observed critical frequencies for the *E*-layer at Tromøya.

MET h m s	*fo*	*MET* h m s	*fo*	*MET* h m s	*fo*
09 01 48	2.75	11 40 34	2.90 A	14 22 37	(2.50)A
09 04 38	2.75	11 45 40	(2.90)A	14 27 51	(2.60)A
09 07 31	2.80	11 47 50	(2.90)A	14 30 47	2.80 A
09 12 41	2.80	11 51 21	(2.90)A	14 34 38	(2.80)A
09 15 31	2.80	11 56 30	(2.90)A	14 38 58	(2.80)A
09 18 22	2.80	11 59 20	(2.90)A	14 41 49	2.85 A
09 23 36	2.80	12 01 11	(2.90)A	14 44 40	2.85 A
09 26 26	2.80	12 07 23	2.90 A	14 49 55	2.85
09 29 17	2.80	12 10 13	(2.90)A	14 52 44	2.80
09 34 26	2.80	12 13 04	(2.90)A	14 55 35	2.80
09 37 16	2.80	12 18 12	(2.90)A	15 00 49	2.80
09 40 07	2.80	12 21 02	(2.90)A	15 03 39	2.80
09 45 14	2.80 A	12 23 53	(2.90)A	15 06 30	2.80
09 48 04	2.80	12 28 56	(2.85)A	15 11 41	2.80
09 50 55	2.80	12 31 46	(2.85)A	15 14 31	2.80
09 56 05	2.80	12 34 36	(2.80)A	15 17 22	2.80
09 58 55	2.80	12 40 39	(2.75)A	15 22 32	2.75
10 01 46	2.80	12 42 28	(2.70)A	15 25 22	2.75
10 06 52	2.80	12 45 19	(2.70)A	15 28 13	2.75
10 09 42	2.80	12 49 49	(2.65)A	15 33 24	2.75
10 12 33	2.80	12 54 01	(2.60)A	15 36 13	2.75
10 17 47	2.80	13 01 33	(2.55)A	15 39 05	2.75
10 20 37	2.80	13 04 22	(2.50)A	15 46 25	2.75 A
10 23 25	2.80	13 06 10	(2.40)A	15 49 15	2.75 A
10 28 42	2.80	13 12 13	(2.30)A	15 52 06	2.75 ZA
10 31 32	2.80	13 15 02	(2.25)A		A
10 34 23	2.80	13 17 50	(2.15)A		A
10 39 47	2.80	13 22 52	(2.10)A		A
10 42 37	2.80	13 25 39	(2.00)A		A
10 45 28	2.80	13 28 27	(1.90)A	16 10 58	2.70
10 50 49	2.85	13 32 52	(1.75)A	16 13 49	2.70
10 53 39	2.85		A	16 18 55	2.70 H
10 56 29	2.85		A	16 21 45	2.70
11 01 52	2.85		A	16 24 34	2.65 H
11 04 42	2.85		A	16 29 38	2.65 H
11 07 33	2.85		A	16 32 28	2.65
11 12 57	2.85 A	13 54 49	(2.05)A	16 35 18	2.60
11 15 48	2.90	13 57 31	(2.10)A	16 40 26	2.60
11 17 59	2.90	14 00 23	(2.15)A	16 43 16	2.60
11 23 58	2.90	14 05 53	(2.25)A	16 46 07	2.60
11 26 47	2.85	14 08 44	(2.30)A	16 51 15	2.60 H
11 29 39	2.90 A	14 11 35	(2.30)A	16 54 03	2.55 H
11 34 53	2.90 A	14 16 53	(2.40)A	16 . 6 56	2.60
11 37 43	2.90 A	14 19 46	(2.50)A		

Table (2.2). Observed critical frequencies for the *E*-layer at Kjeller.

MET h m s	*fo*	*MET* h m s	*fo*	*MET* h m s	*fo*
09 00 18	2.70	11 44 58	(2.75)A		A
09 04 52	2.70	11 49 35	(2.75)A		A
09 09 26	2.70	11 54 12	(2.70)A		A
09 13 59	2.70	11 58 49	(2.70)A	14 43 31	(2.60)A
09 18 32	2.70	12 03 25	(2.65)A	14 47 06	(2.65)AZ
09 23 04	2.65	12 08 02	(2.65)A	14 52 41	(2.70)AZ
09 27 37	2.65	12 12 40	(2.65)A	14 57 11	(2.60)AZ
09 32 10	2.65		A	15 01 45	(2.60)AZ
09 36 43	2.65	12 21 54	(2.60)A	15 06 20	(2.60)AZ
09 41 17	2.65	12 26 33	(2.65)A		A
09 45 50	2.65	12 31 09	(2.65)A	15 15 29	2.65 Z
09 50 24	2.65	12 35 44	(2.60)A	15 20 01	2.60 Z
09 54 57	2.65	12 40 17	(2.50)A	15 24 35	2.60 Z
09 59 30	2.65	12 44 51	(2.50)A		A
10 04 04	2.65	12 49 26	(2.50)A	15 33 43	2.65
10 08 37	2.65	12 54 00	(2.45)A	15 38 17	2.60 H
10 13 10	2.65	12 58 33	(2.40)A	15 42 50	2.60
10 17 43	2.65	13 03 05	(2.35)A	15 47 24	2.60
10 22 36	2.65		A		B A
10 26 49	2.65	13 12 11	(2.25)A		B A
10 31 23	2.65	13 16 43	(2.20)A	16 01 05	2.55
10 35 56	2.65		A	16 05 42	2.60
10 40 32	2.65 A	13 25 44	(2.00)A	16 10 16	2.55
10 45 08	2.70 A	13 30 17	(2.00)A	16 14 52	2.55
10 49 44	2.70 A	13 34 49	(2.00)A		A
10 54 17	2.70	13 39 23	(2.00)A	16 24 02	2.50
10 58 52	2.70 A	13 43 56	(2.00)A		A
11 03 27	2.70 A	13 48 34	(2.10)A		A
11 08 03	2.75 A	13 53 06	(2.10)A		A
11 12 38	2.75 A	13 57 42	(2.20)A		A
11 17 13	2.75 A	14 02 16	(2.20)A		A
11 21 50	2.75 A	14 06 52	(2.25)A	16 51 37	2.50
11 26 27	2.75 A	14 11 26	(2.30)A	16 56 12	2.50
11 31 05	(2.75)A	14 16 02	(2.35)A	17 00 47	2.50
11 35 43	(2.75)A	14 21 27	(2.45)A	17 05 12	2.45
11 40 21	(2.75)A	14 25 12	(2.50)A		

Table (2.3). Observed critical frequencies for the *E*-layer at Tromsø.

MET h m s	*fo*	*MET* h m s	*fo*	*MET* h m s	*fo*
09 02 01	3.95	11 41 11	4.10	14 19 48	3.60 H
09 04 52	3.95	11 44 01	4.10	14 22 39	3.65 H
09 07 42	3.95	11 48 54	4.10	14 27 35	3.75 H
09 12 07	3.90	11 51 47	4.10 H	14 30 25	3.77
09 14 58	3.95	11 54 39	4.10 H	14 33 16	3.80 H
09 17 48	3.95	11 57 29	4.10 H	14 38 09	3.85
09 22 12	3.95	12 02 25	4.10 H	14 41 00	3.90
09 25 03	3.95	12 05 17	4.15 H	14 43 50	3.95
09 27 54	4.00	12 08 06	4.15 HA	14 48 43	3.98
09 33 26	3.95	12 13 00	4 15 H	14 51 33	4.00
09 36 17	3.95	12 15 50	4.15 H	14 54 26	4.00
09 39 07	4.00	12 18 41	4.15	14 59 18	4.00
09 44 08	4.00 H	12 23 37	4.15	15 02 08	4.00
09 46 59	4.00 H	12 26 30	4.15	15 04 58	4.00
09 49 48	4.00 H	12 30 18	4.05	15 09 54	4.02 H
09 55 33	4.05 H	12 35 08	4.00	15 12 46	4.05
09 58 24	4.05 H	12 37 57	3.95	15 15 38	4.00
10 01 14	4.05 H	12 40 46	3.90		L
10 05 37	4.00 PA	12 45 41	3.85 H		L H
10 08 28	[4.00]A	12 48 32	3.80 H		L
10 11 19	4.00	12 51 21	3.75 H		L
10 16 16	4.00	12 56 20	3.70		L H
10 19 06	4.00	12 59 11	3.65		L H
10 21 56	4.00 H	13 02 01	3.55	15 41 58	4.00
10 26 53	4.00 H	13 06 55	3.45	15 44 50	4.00
10 29 44	4.00	13 09 44	3 40	15 47 41	3.97 H
10 32 34	4.00 H	13 12 34	3.30	15 52 41	3.97
10 37 31	4.00	13 17 18	3.17	15 55 31	3.95
10 40 21	4.00	13 20 07	3.03	15 58 23	4.00 H
10 43 11	4.00 H	13 24 51	2.85	16 03 21	3.95 H
10 48 06	4.00 H	13 27 39	2.75 HS	16 06 12	4.00
10 50 56	4.00 H	13 30 34	2.58 H	16 09 01	3.95
10 53 47	4.00 H	13 35 11	2.34 H	16 14 03	3.92
10 58 43	4.05 H	13 37 57	2.17 H	16 16 53	3.90
11 02 33	4.05 H	13 40 45	2.04	16 19 45	3.90
11 04 25	[4.05]PA	13 44 29	2.42	16 24 44	3.88
11 09 23	4.05	13 47 24	2.55 H	16 27 35	3.85
11 12 13	4.05	13 50 21	2.70 H	16 30 25	3.80
11 15 03	4.05	13 55 20	2.93	16 35 22	3.80 L
11 19 59	4.05	13 58 13	3.00	16 38 13	3.82 L
11 22 49	4.05	14 01 05	3.05	16 41 02	3.80 L
11 25 39	4.00	14 06 07	3.18		L
11 30 33	4.10	14 09 08	3.30		L
11 33 23	4.10	14 11 59	3.35		L H
11 36 14	4.10	14 16 56	3.42		L H

Table (2.4). Observed critical frequencies for the F_1-layer at Tromøya.

MET h m s	fo	MET h m s	fo	MET h m s	fo
	A	11 41 04	4.10	14 23 12	3.60
	A	11 46 10	4.10	14 28 24	3.75 H
	A	11 48 21	4.15	14 31 15	3.80 PH
	A	11 51 51	4.10	14 34 07	3.85 H
	A	11 57 00	4.10	14 39 27	3.90
	A	11 59 50	4.10	14 42 19	4.00
	A	12 02 41	4.10 H	14 45 10	4.00 H
	A	12 07 53	4.10	14 50 25	4.00 H
	A	12 10 43	4.10	14 53 15	4.05 H
	A	12 13 35	4.15 H	14 56 06	4.05 H
	A	12 18 43	4.15 H	15 01 20	4.05
	A	12 21 33	4.15 H	15 04 10	4.05
	A	12 24 24	4.15 H	15 07 01	4.05
09 48 35	4.00	12 29 27	4.10 H	15 12 12	4.03
	A	12 32 16	4.05 H	15 15 02	4.00
09 56 36	4.05	12 35 07	4.05 H	15 17 53	4.00
09 59 26	4.05	12 40 12	4.00 H	15 23 05	4.00
10 02 17	4.05	12 43 00	3.90 H	15 25 56	4.00
10 07 23	4.05	12 45 53	3.90 H	15 28 46	(4.00)LH
10 10 13	4.05	12 50 22	3.80	15 33 57	(4.00)LH
10 13 05	4.10	12 54 34	3.75 H	15 36 47	(4.05)L
10 18 19	4.10	13 02 06	3.55 H	15 39 38	(4.05)L
10 21 08	4.05	13 04 55	3.50 H	15 46 57	(3.95)L
	A	13 07 45	3.40 H	15 49 48	(4.00)L
10 29 15	4.15	13 12 49	3.27 H	15 52 39	(4.00)L
10 32 04	4.10	13 15 39	3.23 H	15 57 50	[4.00]L
	A	13 18 17	3.12 H	16 00 40	4.05 H
	A	12 23 19	3.03 H	16 03 31	4.00 H
	A	13 26 06	2.93	16 08 41	3.95 H
	A	13 28 53	2.82 H	16 11 31	3.95 H
	A	13 33 15	2.57 H	16 14 22	3.95 H
	A	13 36 02	2.45 H	16 19 27	3.90 H
10 57 05	4.05	13 38 50	2.36 H	16 22 17	3.90
11 02 22	4.05	13 44 02	2.38 H	16 25 08	3.85
11 05 12	4.05	13 46 58	2.53 H	16 30 12	3.85
11 08 04	4.10	13 49 51	2.68 P	16 33 06	3.90
11 13 28	4.10	13 55 14	2.93 P	16 35 53	3.90 H
11 16 18	4.10	13 57 56	3.01	16 41 01	3.90
11 18 29	4.10	14 00 50	3.10 P	16 43 51	3.85 L
11 24 28	4.10	14 06 31	(3.30)H	16 46 41	3.80 L
11 27 18	4.10	14 09 21	3.35 H	16 51 49	3.80 L
11 30 09	4.10	14 12 13	3.40 H	16 54 38	(3.75)L
11 35 23	4.10	14 17 30	3.53 H		L H
11 38 13	4.10	14 20 21	3.60 H		

Table (2 5). Observed critical frequencies for the F_1-layer at Kjeller.

MET h m s	*fo*	*MET* h m s	*fo*	*MET* h m s	*fo*
09 00 50	3.85 Z	11 45 30	3.95 H	14 30 23	(3.80)ZLH
09 05 24	3.90	11 50 06	3.90 HZ	14 34 58	(3.85)LZ
09 09 58	3.90 H	11 54 45	3.95 HZ	14 39 33	(3.90)LZ
09 14 30	3.80 H	11 59 23	4.00 H	14 44 06	(3.90)LZH
09 19 03	3.80	12 03 59	3.90 Z	14 48 49	(3.90)LH
09 23 38	3.85 H	12 08 36	3.90 H	14 53 13	(3.90)LZH
09 28 11	3.90 H	12 13 15	3.95 H	14 57 46	3 90 Z
09 32 44	3.90 H	12 17 53	3.95 H	15 02 20	3.90 L
09 37 17	3.90 H	12 22 30	3 95 H	15 06 55	(3.90)L
09 41 51	3.90 H	12 27 08	3.95 H	15 11 29	(3.90)L
09 46 24	3.90 H	12 31 44	3.95 H	15 16 03	3.90 LZ
09 50 58	3.90 H	12 36 19	3.90	15 20 36	3.85
09 55 31	3.90 H	12 40 55	3.85 H	15 25 10	3.85 H
10 00 05	3.95 H	12 45 27	3.75 H	15 29 43	3.85 H
10 04 39	3 95 H	12 50 01	3.65 H	15 34 16	3.80 H
10 09 12	3.95 H	12 54 36	3.60 H	15 38 51	3.85 H
10 13 45	3.95 H	12 59 10	3.55	15 43 24	3.80 H
10 18 18	3.95 H	13 03 42	3.50 H	15 47 58	(3.80)LZ
10 22 52	4.00 H	13 08 16	3.40 H	15 52 33	(3.85)L
10 27 24	3.95 H	13 12 49	3.35 H	15 57 07	3.80
10 31 57	3.90 H	13 17 21	3.20 H	16 01 41	3.80
10 36 30	3.90 HZ	13 21 44	3.15 H	16 06 15	3.75
10 41 06	3.90 Z	13 26 15	3.10	16 10 51	3.75
10 45 40	3.90 Z	13 30 47	3.05	16 15 27	3.70
10 50 16	3.90 Z	13 35 19	3.03	16 20 03	(3.80)L
10 54 50	3.95	13 39 51	3.00		L
10 59 25	3.95 H	13 44 26	3.05		L
11 04 00	3.95 HZ	13 49 02	3.10		L
11 08 35	3.95 H	13 53 46	3.20 H		L
11 13 10	3.95 HZ	13 58 22	3.35		L
11 17 46	4.00 H	14 02 57	3.40	16 47 37	(3.70)L
11 22 23	4.00 H	14 07 32	3.50 Z	16 52 13	(3.70)L
11 27 00	4.00 H	14 12 06	3.55 Z		L
11 31 37	3.95 Z	14 16 41	3.65 H		L
11 36 14	3.90 Z	14 21 14	3.70 H	17 05 59	(3.75)L
11 40 53	3.95	14 25 48	3.75 HL		

Table (2.6). Observed critical frequencies for the F_1-layer at Tromsø.

MET h m s	*fo*	*MET* h m s	*fo*	*MET* h m s	*fo*
09 02 13	4.90	11 41 27	5.25	14 19 52	3.87
09 05 06	4.95	11 44 15	5.20	14 22 42	3.93
09 07 56	4.95	11 49 07	5.10	14 27 39	4.05
09 12 21	4.95	11 52 01	5 10	14 30 29	4.10
09 15 12	5 00	11 54 52	5.10	14 33 21	4.15
09 18 02	5.00	11 57 43	5.10	14 38 14	4.25
09 22 25	4.90	12 02 36	4.95	14 41 05	4.32
09 25 17	5.00	12 05 27	4.95	14 43 55	4.32
09 28 07	5.00	12 08 15	4.90	14 48 48	4.40
09 33 38	4.90	12 13 09	4.80	14 51 39	4.50
09 36 30	4.95	12 15 58	4.75	14 54 32	4.50
09 39 19	4.95	12 18 47	4.65	14 59 24	4.50
09 44 19	4.90	12 23 43	4.60	15 02 14	4.50
09 47 10	4.90	12 26 35	4.55	15 05 04	4.50
09 49 59	4.85	12 30 24	4.50	15 10 00	4.47
09 55 44	4.85	12 35 12	4.35	15 12 50	4.42
09 58 35	4.85	12 38 02	4.30	15 15 43	4.40
10 01 25	4.85	12 40 51	4.25 F	15 20 40	4.40
10 05 48	4.85	12 45 46	4.23	15 23 32	4.40
10 08 39	(4.85)A	12 48 38	4.20	15 26 21	4.30
10 11 30	4.85	12 51 27	4.15	15 31 19	4.25
10 16 27	4.90	12 56 25	4.10	15 34 08	4.20
10 19 18	4.95	12 59 16	4.08	15 36 59	4.15
10 22 08	4.95	13 02 07	4.00	15 42 02	4.30
10 27 07	5.05	13 07 02	3.95	15 44 54	4.32
10 29 58	5.10	13 09 51	3.93	15 47 46	4.33
10 32 48	5.10	13 12 42	3.90	15 52 45	4.35
10 37 45	5.10	13 17 36	3.80	15 55 37	4.34
10 40 36	5.10	13 20 27	3.75	15 58 27	4.33
10 43 26	5.15	13 25 17	3.70	16 03 26	4.30
10 48 21	5.20	13 28 07	3.65	16 06 16	4.30
10 51 11	5.20	13 30 55	3.55	16 09 06	4.33
10 54 04	5.25	13 35 48	3.45	16 14 10	4.40
10 58 59	5.30	13 38 38	3.35	16 17 00	4.40
11 02 49	5.25	13 41 29	3.30	16 19 51	4.40
11 04 42	5.30	13 45 00	3.20	16 24 51	4.40
11 09 40	5.40	13 47 52	3.25	16 27 41	4.35
11 12 31	5.40	13 50 45	3.30	16 30 33	4.40
11 15 21	5.40	13 55 38	3.30	16 35 30	4.33
11 20 18	5.50	13 58 29	3.30	16 38 20	4.27
11 23 09	5.55	14 01 21	3.40	16 41 10	4.35 H
11 25 59	5.55	14 06 20	3.50	16 46 07	4.40
11 30 52	5.45	14 09 12	3.60	16 48 57	4.35
11 33 42	5.45	14 12 04	3.70	16 51 48	4.35
11 36 32	5.40	14 17 01	3.80	16 56 47	4.32

Table (2.7). Observed critical frequencies for the F_2-layer at Tromøya.

MET h m s	*fo*	*MET* h m s	*fo*	*MET* h m s	*fo*
09 02 32	4.90	11 41 19	5.25	14 23 17	4.00 P
09 05 21	4.80 A	11 46 24	5.15	14 28 28	[4.05]B
09 08 13	4.85 A	11 48 34	. 5.15	14 31 19	4.10
09 13 24	4.95 A	11 52 04	5.10	14 34 11	4.20
	A	11 57 13	5.10	14 39 33	4.28
	A	12 00 04	5.15	14 42 23	4.30
09 24 19	4.95	12 02 54	5.10	14 45 14	4.30
09 27 08	4.90	12 08 06	5.05	14 50 31	4.45
	A	12 10 55	5.00	14 53 21	4.50
09 35 06	4.80	12 13 44	4 90	14 56 12	4.50
09 37 59	4.95	12 18 57	4.80	15 01 27	4.55
09 40 50	4.95	12 21 41	4.75	15 04 17	4.55
09 45 57	4.95	12 24 31	4.70	15 07 07	4.45
09 48 46	4.90	12 29 34	4.58	15 12 18	4.45
09 51 37	4.90	12 32 23	4.55	15 15 07	4.40
09 56 47	4.85	12 35 13	4.50	15 17 58	4.40
09 59 36	4.80	12 40 17	4.40	15 23 09	4.35
10 02 27	4.80	12 43 06	4.35	15 25 59	4.30
10 07 33	4.75	12 45 57	4.30	15 28 50	4.35
10 10 23	4.75	12 50 28	4.25	15 34 01	4.30
10 13 14	4.75	12 54 40	4.15	15 36 51	4.30
10 18 28	4.80	13 02 13	4.10	15 39 41	4.25
10 21 18	4.75	13 05 03	4.08	15 47 01	4.25
10 24 07	4.85	13 07 53	4.05	15 49 51	4.25
10 29 24	4.90	13 12 57	3.92	15 52 42	4.25
10 32 15	4.95	13 15 47	3.85,	15 57 52	4.20
10 35 07	5.00	13 18 34	3.75	16 00 43	4.25 P
10 40 32	5.10	13 23 38	3.60	16 03 35	4.30
10 43 22	5.10	13 26 27	3.55	16 08 46	4.30
10 46 14	5.15	13 29 32	3.52	16 11 36	4.30
10 51 33	5.10	13 33 43	3.43	16 14 27	4.35
10 54 23	5.10	13 36 35	3.40	16 19 32	4.25
10 57 15	5.15	13 39 26	3.38	16 22 23	4.35
11 02 37	5.20	13 44 36	3.30	16 25 15	4.40
11 05 27	5.20	13 47 26	(3.35)JP	16 30 19	4.40
11 08 20	5.30	13 50 17	3.28	16 33 10	4.45
11 13 44	5.30	13 55 33	3.30	16 35 59	4.35
11 16 34	5.30	13 58 13	3.30	16 41 05	4.20
11 18 44	5.25	14 01 05	3.40	16 43 56	4.25
11 24 44	5.30	14 06 33	3.50	16 46 46	4.20
11 27 34	5.30	14 09 24	3.55	16 51 56	4.30
11 30 25	5.30	14 12 17	[3.70]B	16 54 46	4.30
11 35 39	5.30	14 17 33	3.80	16 57 37	4.30
11 38 29	5.30	14 20 24	3.90		

Table (2.8). Observed critical frequencies for the F_2-layer at Kjeller.

MET h m s	*fo*	*MET* h m s	*fo*	*MET* h m s	*fo*
09 01 00	4.60 Z	11 45 38	4.55	14 30 24	3.92 Z
09 05 33	4.55	11 50 16	4.65 Z	14 34 59	3.95 Z
09 10 08	4.60	11 54 54	4.65 Z	14 39 34	4.00 Z
09 14 40	4.55	11 59 32	4.70	14 44 08	4.05
09 19 12	4.50	12 04 11	4.75 Z	14 48 43	4.10
09 23 47	4.55	12 08 48	4.80	14 53 16	4.10 Z
09 28 20	4.55	12 13 24	4.65	14 57 50	4.15
09 32 52	4.50	12 18 03	4.70	15 02 24	4.20
09 37 25	4.50	12 22 41	4.75	15 06 59	4.20
09 41 59	(4.50)FV	12 27 19	4.75	15 11 33	4.15
09 46 32	(4.50)FV	12 31 53	4.65	15 16 07	4.15 Z
09 51 07	4.55	12 36 29	4.60	15 20 40	4.15
09 55 41	4.60	12 41 04	4.55	15 25 14	4 15
10 00 14	4.60	12 45 37	4.45	15 29 47	4.20
10 04 46	4.50	12 50 10	4.35	15 34 21	4.20
10 09 19	4.50	12 54 45	4.30	15 38 56	4.25
10 13 54	4.60	12 59 18	4.20	15 43 29	4.20
10 18 27	4.60 F	13 03 50	4.10	15 48 02	4.10
10 22 58	4.50 F	13 08 25	4.10	15 52 34	3.95
10 27 31	4.50 Z	13 12 58	4.00	15 57 10	(4.00)F
10 32 07	4.60	13 17 30	3.90	16 01 46	4.15
10 36 38	4.50 Z	13 22 03	3.85	16 06 21	4.20
10 41 12	4.50 Z	13 26 34	3.75	16 10 59	4.30
10 45 50	4.60 Z	13 31 07	3.70	16 15 34	4.25
10 50 26	4.65 Z	13 35 38	3.63	16 20 09	4.25
10 54 59	4.60	13 40 12	3.60	16 24 44	4.15
10 59 34	4.60	13 44 45	3.60	16 29 19	4.10
11 04 09	4.60	13 49 20	3.65	16 33 53	4.05
11 08 42	4.45	13 53 53	3.68	16 38 29	4 05 Z
11 13 17	4.45 Z	13 58 26	3.64	16 43 06	4.10
11 17 51	4.40	14 03 01	3.70 Z	16 47 42	4.10
11 22 28	4.40	14 07 35	3.75	16 52 19	4.15
11 27 05	4.40	14 12 10	3.90	16 56 54	4.15
11 31 44	4.45	14 16 44	3.88	17 01 29	4.15
11 36 22	4.50	14 21 15	(3.82)JF	17 06 04	4.10
11 41 01	4.55	14 25 50	3.87		

Table (2.9). Observed critical frequencies for the F_2-layer at Tromsø.